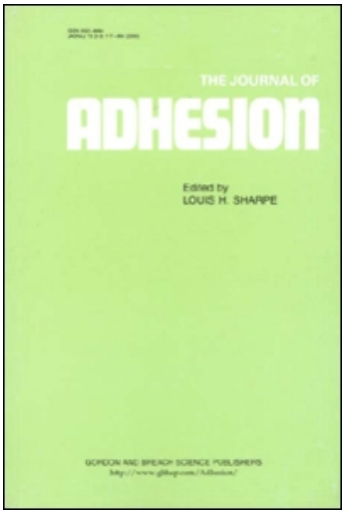

The Journal of Adhesion
Publication details, including instructions for authors and subscription information:
http://www.informaworld.com/smpp/title~content=t713453635

The Electrochemistry of the FPL (Forest Products Laboratory) Process and its Relationship to the Durability of Structural Adhesive Bonds

A. V. Pocius[a]
[a] 3M/Adhesive Technology Center, St. Paul, MN, U.S.A.

To cite this Article Pocius, A. V.(1992) 'The Electrochemistry of the FPL (Forest Products Laboratory) Process and its Relationship to the Durability of Structural Adhesive Bonds', The Journal of Adhesion, 39: 2, 101 — 121
To link to this Article: DOI: 10.1080/00218469208026543
URL: http://dx.doi.org/10.1080/00218469208026543

J. Adhesion, 1992, Vol. 39, pp. 101–121
Reprints available directly from the publisher
Photocopying permitted by license only

Printed in the United States of America.

The Electrochemistry of the FPL (Forest Products Laboratory) Process and its Relationship to the Durability of Structural Adhesive Bonds*

A. V. POCIUS

3M/Adhesive Technology Center, St. Paul, MN 55144-1000, U.S.A.

(Received July 24, 1991; in final form November 4, 1991)

The FPL (Forest Products Laboratories) Process for preparing aluminum for structural adhesive bonding has been used in the aerospace industry since the early 1950's. Problems were encountered with the use of the process when the industry changed from phenolic to epoxy adhesives. In-service disbonds followed by corrosion were observed. This review article describes an investigation of the electrochemistry of the FPL etch process. Through a combination of electrochemical polarization measurements, surface chemical and surface morphological investigations and a thorough application of the Boeing wedge test, we are able to provide a mechanism of action of the FPL etch process. An oscillating electrochemical reaction was observed for low alloy aluminum which was ascribed to the dissolution and redeposition of copper on the aluminum during the etching process. A spatial variation in wedge test performance was found in that edge specimens demonstrated lower crack extensions than center specimens when using a low alloy aluminum that was etched in an FPL etch bath that was low in copper. These results are positioned in a historical perspective providing some insight into possible reasons for the irreproducibility of durability of structural adhesive bonds made with low alloy aluminum adherends that were prepared in a low copper content FPL etch bath.

KEY WORDS etch; FPL; Forest Products Laboratory; sulfuric/chromic; surface; surface preparation; adhesion; durability; structural; aluminum; adhesive.

INTRODUCTION

The durability of structural adhesive bonded joints is now well known to be dependent upon the surface preparation of the adherends and the surface oxide chemistry and structure that is created thereby.[1] This is particularly true for the structural adhesive bonding of aluminum adherends. Much of the fundamental understanding relating aluminum oxide chemistry and morphology to the durability of structural adhesive bonds stems from the work of Venables and his group.[2,3] It is fitting that this article be included in this special issue of the Journal of Adhesion, since the

*One of a Collection of papers honoring John D. Venables, the recipient in February 1991 of *The Adhesion Society Award for Excellence in Adhesion Science, Sponsored by 3M.*

work described herein was inspired by the investigations of John Venables and his research group at the Martin-Marietta Research Laboratory.

The FPL (Forest Products Laboratory) Etch[4] is the first widely used surface preparation procedure for aluminum structural adhesive bonding. The FPL etch is a solution of a dichromate salt in sulfuric acid. In the process, the etch is usually preceded by an alkaline detergent bath to remove gross amounts of grease and is anteceded by a rinse bath, usually using tap water. Variants in the etch procedure are the temperature (usually elevated above ambient), the etching time, the type of rinse water, the type of dichromate salt and the level of contaminants in the bath whether added purposefully or as a result of the etching process itself. In the U.S., the etch bath generally consists of a solution of 30 parts of deionized water, 10 parts of sulphuric acid and 1 to 2 parts of sodium dichromate, all by weight. The bath is usually held at 160°F (71°C) and the etching time is usually 10 minutes. The rinse water is normally tap water. In Europe, the etch is often referred to as "pickling," and frequently chromic acid is substituted for sodium dichromate, the etching time is often longer and the rinse water is often specified to be deionized. These statements are meant to be general descriptions; there are probably as many variations in the procedure as there are manufacturers of aluminum adhesively bonded parts.

In the early 1960's, as manufacturers of aircraft moved to the use of epoxy adhesives, supplanting the harder-to-use phenolic adhesives, a problem was discovered in that adhesive bonds were failing in service at relatively short times. The failure was followed by general corrosion of the part, possibly accelerated by the fact that a crevice was created as a result of the delamination. This phenomenon was discussed by Sharpe,[5] McMillan[1] and Bethune.[6] The problems occured mostly in bilge areas under galleys and toilets and also in adhesively bonded honeycomb sandwiches. The surface preparation procedure used at that time was the FPL etch. The discovery of the source of the problem was made more difficult in that not all adhesive bonds failed at short times; rather, some bonds lasted for quite long times. The Boeing Company launched a major research program in this area to discover the reasons for the premature failures as well as the irreproducibility. There were three major results of this research program: the Boeing wedge test for predicting durability of structural joints,[7] the phosphoric acid anodization procedure[8] and the "optimized" FPL etch. The chemistry of the "optimized" FPL etch is only slightly changed from the original FPL etch. The major departure in chemistry was the introduction of a small amount of predissolved 2024-T3 aluminum alloy. The addition of the 2024-T3 alloy to generate the "optimized" etch is also known as "seeding" of the bath. Seeding of the FPL etch bath with this alloy decreased the irreproducibility of durability for aluminum structural adhesive bonded joints.

The research of Venables *et al.*[2,3] was mostly concerned with the oxide chemistry and morphology produced by commercial anodization methods. Some of their work was concerned with the FPL etch process.[3] We saw the need for a deeper understanding of the effect of "seeding" of the FPL etch solution as it concerned the reasons for irreproducible durability when the FPL etch process was used for structural adhesive bonding of aluminum for aerospace use. Some work on the FPL etch process had been done previous to our work by Smith,[9] Bijlmer,[10] Russell and Garnis,[11] Wegman, *et al.*[12] and McGarvill and Bell.[13] The overall understanding of

the FPL etch process was more recently reviewed by Kozma and Olejford.[14] It is the purpose of this article to review the 3M work in this area[15] and to provide our concept of the reasons for the historical irreproducibility of bonded joints made using aluminum etched by the FPL process.

FPL ETCH ELECTROCHEMISTRY

Electrochemical Methods

The use of electrochemical techniques such as polarization measurements to study electrode reactions is well known in the literature.[16] The pertinent features of an electrochemical polarization measurement are shown in Figure 1. The polarization

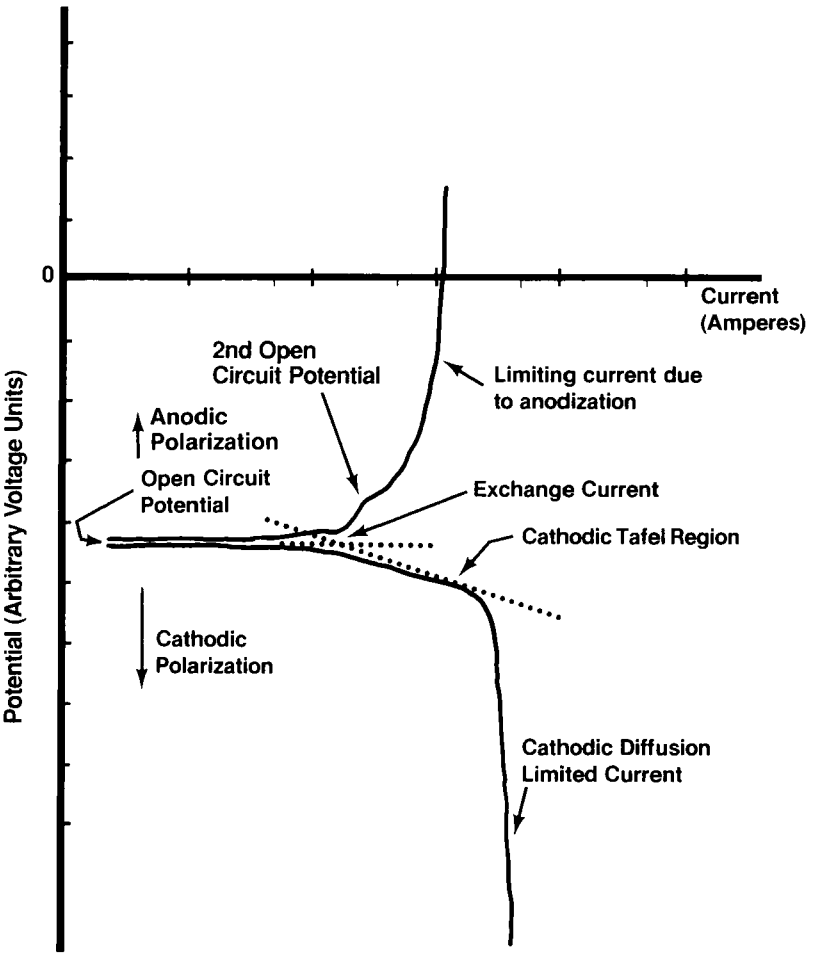

FIGURE 1 Schematic diagram of features in an electrochemical polarization curve. (From Reference 9a. Reprinted by permission of SAMPE.)

curve in this figure, although similar to those measured in this work, is meant to be illustrative of the general features of a polarization curve. Hence, the axes have arbitrary units. The vertical axis is potential *versus* a standard electrode. The horizontal axis is the logarithm of the current flowing through the cell. The **open circuit potential** is that which is measured between the Standard Calomel Electrode (SCE) and the working electrode under conditions of no applied voltage or current. An open circuit potential that varies with time is indicative of an electrode that is not in equilibrium with its surroundings. The **exchange current** is the current which flows between the anodic and cathodic sites on a metal surface under open circuit conditions. The exchange current is proportional to the rate of the electrochemical reactions occuring at the working electrode surface under open circuit conditions. The **Tafel region** is the portion of a semilogarithmic polarization plot that represents electron transfer control and is sufficiently far from the open circuit potential to be linear. Extrapolation of a Tafel region to zero applied potential results in a measurement of the exchange current. **Diffusion limited current** occurs when the rate of the electrode reaction depends upon the rate of arrival of the reactants at the electrode surface.

Experimental

Surface Treatment The bath compositions and conditions were as follows: 1. Alkaline degrease – 75 g. of Oakite 164 (alkaline detergent) per liter of distilled water, maintained at 85–92°C. 2. FPL Etch. "Fresh" FPL etch solutions were made up to be 0.123 M in chromate ion using $Na_2Cr_2O_7 \cdot 2H_2O$ and 6.15 M in H^+ using concentrated H_2SO_4. Distilled water having less than 1.0 ppm total dissolved salts was used in all cases. The "optimized" or "seeded" FPL etch bath was made from 1161 g of concentrated H_2SO_4, 156.8 g of sodium dichromate, 1.5 g of 2024-T3 bare aluminum alloy chips and distilled water to make 3.5 liters. Experimental solutions to determine the effect of various constituents of the etch bath were made up having the concentration of the ingredients equivalent to those in the "optimized" etch. 3. Tap water rinse. Ambient temperature water from a laboratory faucet was used for the rinse steps.

In this work, the typical surface treatment was as follows: (1) acetone wipe, (2) 10 min alkaline degrease, (3) 1 to 2 minutes tap water rinse, (4) 10 min in the FPL etch held at 71°C, (5) 1 to 2 minutes tap water rinse, (6) 5 or 10 minutes dry at 66°C. For certain measurements, only the appropriate portion of the surface treatment was carried out.

Metals 2024 alloy is 93.5% aluminum, 4.4% copper, 0.6% manganese and 1.5% magnesium. The cladding or Alclad alloy on the 2024-T3 Alclad material is 1230 alloy which is nominally 99.3% aluminum with the major impurities being silicon and iron (maximum total concentration, 0.7%). The cladding layer is typically 0.0035" (0.09 mm) thick. 1100 alloy has a minimum purity of 99.00%, the main impurity being copper. "T3" refers to the heat temper of the alloy. The source of this information is the Metals Handbook.[17]

Electrochemical measurements The electrochemical measurements were carried out using a PAR/EG&G Potentiostat/Galvanostat with Logarithmic Current Converter and electrometer input. A PAR/EG&G Universal Programmer was used to control the scan rate which, unless otherwise specified, was 0.5 mV/sec. All potentials were measured *versus* the Standard Calomel Electrode (SCE). The electrochemical cell and electrometer were isolated from electrical noise by a Faraday cage. The SCE was isolated from the cell by a Luggin capillary. The working electrode (the aluminum alloy) was contained in a PAR/EG&G K105 Flat Specimen Holder and the counter electrode was graphite. The cut edges of the specimen were NOT exposed to the solution during the electrochemical measurements.

The alloy surfaces were prepared using steps 1–3 as described above. The electrode kinetics of the alloys were determined in the FPL etch solutions at 71°C. The solution was not stirred or deaerated. This was done in order to mimic, as closely as possible, the FPL etch bath as used in production. The time dependence of the open circuit potential was monitored for at least 10 minutes before the electrode was polarized. Anodic and cathodic polarization were performed on different samples, hence the low current portion of the cathodic polarization curve did not always correspond exactly with the low current portion of the anodic curve.

Results and discussion One of the major findings of our work was the discovery of an oscillating electrochemical reaction occurring on the surface of certain aluminum alloys as a function of the amount of predissolved aluminum alloy in the etch bath. This finding is illustrated in Figures 2, 3 and 4. Figure 2 shows the open circuit

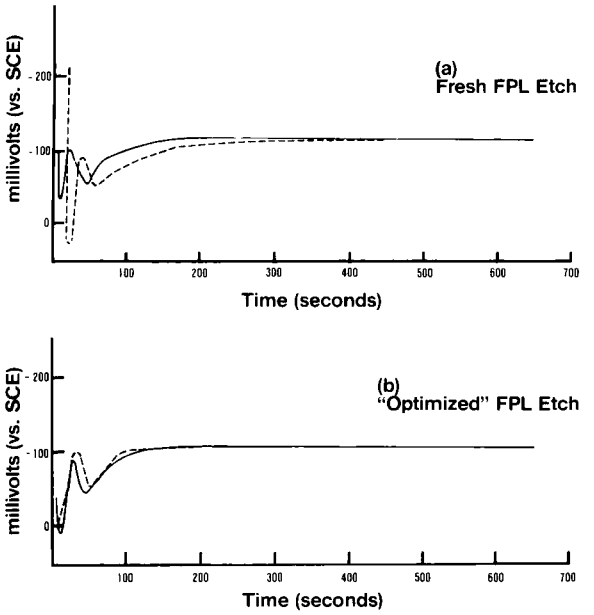

FIGURE 2 Open circuit potential *versus* time for 2024-T3 bare alloy in (a) "fresh" FPL etch solution and (b) "optimized" FPL etch solution. Note that the open circuit potential is at approximately −100 mV and is constant with time. Dashed line is a repeat of the experiment using a new piece of metal for the electrode. (From Reference 9b. Reprinted by permission of Plenum Press.)

potential as a function of time for bare 2024-T3 alloy in fresh and "seeded" FPL etch solution. We note that no oscillations occur even after extended exposure to the solutions. The open circuit potential is approximately −100 mV *vs.* the SCE for 2024-T3 bare alloy in both the fresh and optimized FPL etch. The observation is drastically different for the case of clad 2024-T3 aluminum alloy in the fresh and "optimized" FPL etch baths as shown in Figure 3. At some point in the exposure to the bath, the open circuit potential begins to oscillate approximately between −130 and −250 mV *vs.* SCE. The same phenomenon occurs for 1100 alloy as shown in Figure 4. The 1100 alloy has approximately the same chemical composition as the cladding on clad 2024-T3 alloy. For the 1100 alloy, the oscillations occur approximately between −100 mV and −250 mV. The fact that potential oscillation occurs for both 1100 and clad 2024-T3 alloy indicates that the phenomenon is not due to penetration of the cladding in the case of the clad alloy. It is unrealistic to believe that the FPL solution would etch through 0.0035″ (0.09 mm) of metal during the time of the experiment. The same phenomenon is observed for both 1100 and 2024-T3 alloy in FPL etch solutions in which copper filings have been dissolved

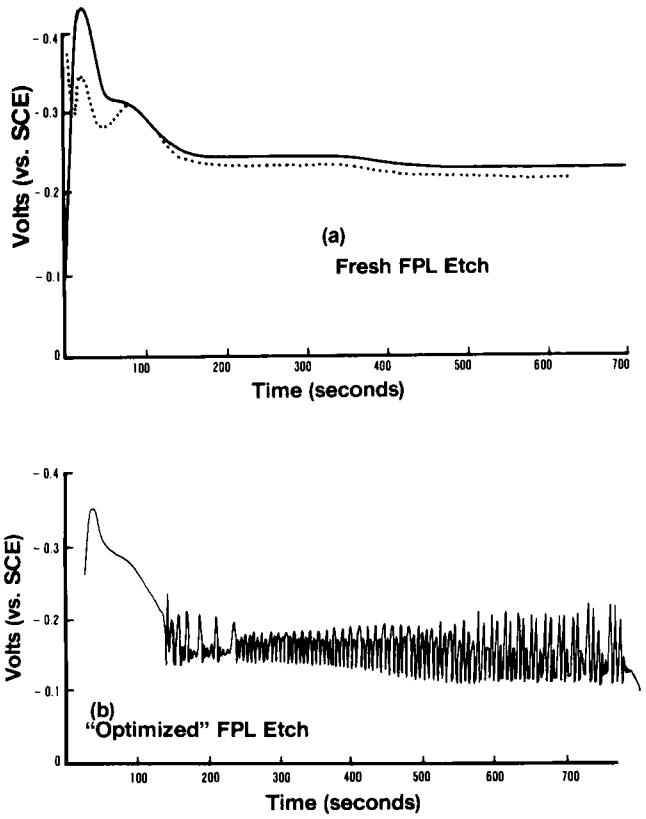

FIGURE 3 Open circuit potential *versus* time for 2024-T3 clad alloy in (a) "fresh" FPL etch solution and (b) "optimized" FPL etch solution. The cut edges of the alloy were **not** exposed to the solution. Note that the open circuit potential for this alloy is constant in the "fresh" etch but exhibits oscillating behavior in the "optimized" etch. Dashed line is a repeat of the experiment using a new piece of metal for the electrode. (From Reference 9a. Reprinted by permission of SAMPE.)

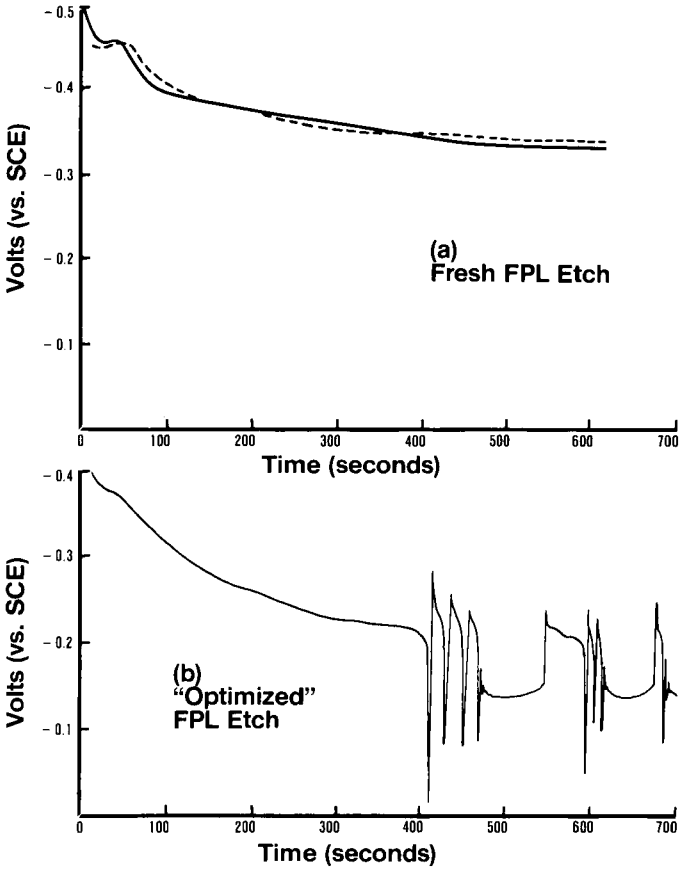

FIGURE 4 Open circuit potential *versus* time for 1100 alloy in (a) "fresh" FPL etch solution and (b) "optimized" FPL etch solution. Note that the open circuit potential for this alloy is constant in the "fresh" etch but exhibits oscillating behavior in the "optimized" etch. Dashed line is a repeat of the experiment using a new piece of metal for the electrode. (From Reference 9a. Reprinted by permission of SAMPE.)

instead of 2024-T3 bare alloy chips. This indicates that it is the absence or presence of copper in the bath that controls the observance of the open circuit potential oscillations. Electrode potential oscillations have been observed for metals other than aluminum[18] and a short synopsis of the phenomenon is given by Vetter.[19] The phenomenon is usually observed for metals which undergo active-passive transitions, and occurs for those metals only when concentration changes occur in the electrolyte during the activation-passivation process.

Some elucidation of the mechanism can be obtained by examining the polarization curves of bare and clad 2024-T3 alloy and 1100 alloy. The polarization curves for 2024-T3 bare alloy are shown in Figure 5. The obvious item to note is that the two curves are seemingly identical. There is only a slight increase in the current draw at any potential for the 2024-T3 bare electrode in the "optimized" FPL solution over that in the "fresh" etch.

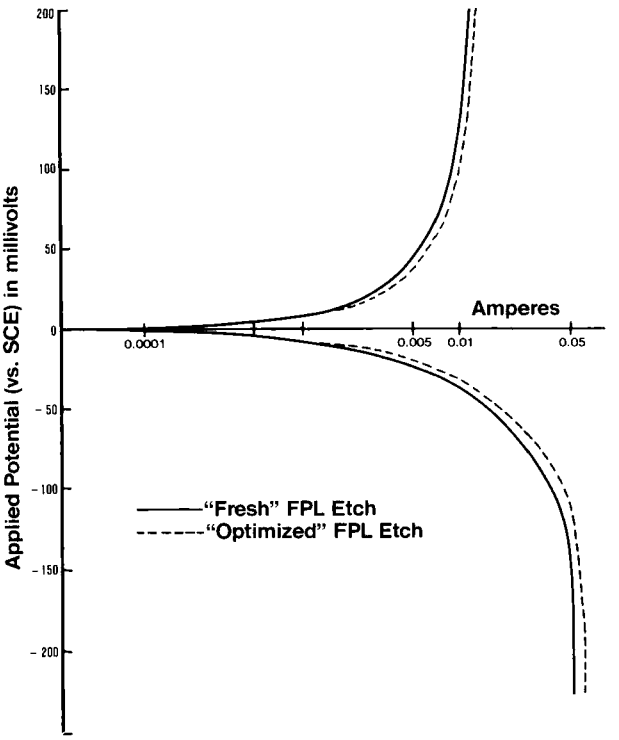

FIGURE 5 Electrochemical polarization curves for 2024-T3 alloy in (——) "fresh" *versus* (- - - -) "optimized" FPL etch. Note that the polarization curves are only slightly different from one another indicating that the exchange current is only slightly different, if at all changed, for this alloy in the two etch baths. (From Reference 9b. Reprinted by permission of Plenum Press.)

Figure 6 shows the polarization curves for clad 2024-T3 alloy in the FPL etch solution as well as in solutions of the components. The polarization curve in dichromate-only solution is essentially featureless showing diffusion limited current at anodic and cathodic potentials. The open circuit potential, which is not very apparent in the figure, is −295 mV *vs.* SCE. The anodic diffusion limited current is likely due to the formation of an anodic oxide. The cathodic diffusion limited current could also be indicative of the formation of an insoluble layer on the electrode surface. Although the shape of the polarization curve of 2024-T3 clad alloy in dichromate solution may seem unrealistic in comparison with polarization curves for other metals, the curve was reproducible. It is well known that chromate salts are particularly good corrosion inhibiting agents for aluminum[20] and this inhibition ability could be due to the limitation of current draw at the cathodic sites as demonstrated by this polarization curve.

The polarization curve for 2024-T3 clad alloy in sulphuric acid, also displayed in Figure 6, shows an anodic diffusion limited current but no cathodic diffusion limited current. Sulphuric acid is a well-known electrolyte for the anodization (electrochemically induced growth of a surface oxide) of aluminum and the anodic diffusion limited current is likely demonstrative of anodization.

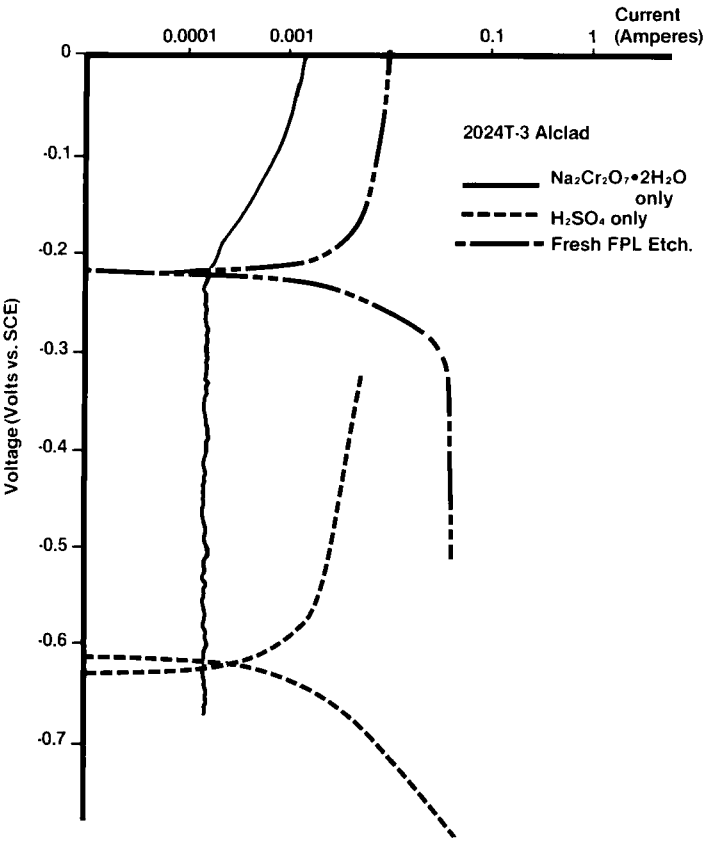

FIGURE 6 Electrochemical polarization curves for 2024-T3 clad alloy in (——) solution containing only sodium dichromate, (- - -) solution containing only sulphuric acid and (- - —— - - —— - -) the "fresh" FPL etch solution. Note that the polarization curve for the "fresh" etch is essentially a superposition of the curves for the components of the etch. (From Reference 9a. Reprinted by permission of SAMPE.)

The polarization curve for 2024-T3 clad alloy in the fresh FPL etch solution, also shown in Figure 6, is a composite of the polarization curves of this alloy in dichromate and sulphuric acid solution. The open circuit potential is much more positive in the FPL etch than it is in sulphuric acid. The anodic portion shows what appears to be a diffusion limited current at high anodic potentials. It is likely that this limited current is due to the formation of an anodic oxide. The cathodic portion shows a break at which the curves change from a charge transfer regime to a diffusion limited current. It is significant that the break in the curve occurs at approximately the open circuit potential (-295 mV vs. SCE) of the working electrode in dichromate only solution. This indicates that as soon as the electrode attains the open circuit potential of the alloy in the dichromate solution, the dichromate reaction, which is limited by diffusion, becomes the dominant reaction.

The data shown in Figure 6 are exemplary of the Wagner-Traud mixed potential theory of electrode reactions.[21] The theory states that the sum of all of the individual redox reactions taking place on an electrode surface will determine the

overall current-voltage dependence, and will define a "mixed" potential at which the sum of all of the anodic currents equals the sum of all of the cathodic currents.

The data taken in these measurements do not allow us to pinpoint the actual chemical reactions taking place at the working electrode surface. We can, however, make reasonable suppositions. Under acidic conditions the likely anodic reaction at the open circuit potential is:

$$Al \longrightarrow Al^{+3} + 3e^{-}. \tag{1}$$

At high anodic potentials, the current is likely limited by the following reaction which deposits an insulating oxide on the surface:

$$2\ Al^{+3} + 3H_3O \longrightarrow Al_2O_3 + 6H_2 \tag{2}$$

Possible cathodic reactions under acidic conditions are:

$$6H^{+} + 6e^{-} \longrightarrow H_2 \tag{3}$$

$$Cr_2O_7^{2-} + 6e^{-} + 14H^{+} \longrightarrow 2Cr^{+3} + 7H_2O \tag{4}$$

$$3/2\ O_2 + 6e^{-} + 6H^{+} \longrightarrow 3H_2O \tag{5}$$

The lack of chromium on FPL etched surfaces[15b] indicates that under open circuit conditions reaction (4) is not the prevalent cathodic reaction. Since oxygen reduction (reaction 5) usually occurs at high potentials, the likely cathodic reaction is reaction (3). Unfortunately, experiments in deaerated solutions were not run because this was considered to be non-realistic in comparison with the way the FPL etch is done in production. We also have to consider reaction (6):

$$Cu^{2+} + 2e^{-} \longleftrightarrow Cu(s) \tag{6}$$

because the addition of copper to the FPL etch bath has such a pronounced effect on the time dependence of the open circuit potential of the pure and clad alloy.

Figure 7 shows the polarization results for 1100 alloy in the FPL etch. The solid line represents measurements in the fresh FPL etch solution and the dotted line those in the optimized FPL etch solution. For comparison, the data for the 2024-T3 bare alloy in the optimized etch are also included. The 1100 alloy demonstrated cathodic Tafel regions whose slope changed in going from the fresh to the optimized FPL etch. The Tafel regions for this system are decidedly short. However, this difference in slope was reproducible from sample to sample. No conclusion is drawn from the actual value of the slope. Rather, the significance of the measurement is that the slope changes. The change in slope indicates a change in the charge transfer reaction between the fresh and optimized etch. Also noted in Figure 7 is a "bump" at about -180 mV in the anodic polarization of the 1100 alloy in the optimized etch. In several measurements, this "bump" became another open circuit potential at about -180mV. We have no explanation as to why this second open circuit potential was not always seen for these experimental conditions. If the second open circuit potential was not seen, the "bump" was seen. The element added to the FPL etch solution which is most likely to exhibit this phenomenon on aluminum is copper. We believe that the 2nd open circuit potential observed corresponds to the mixed potential caused by the existence of reaction (6) in systems containing copper. Copper is more noble than aluminum and it is expected to electroplate on

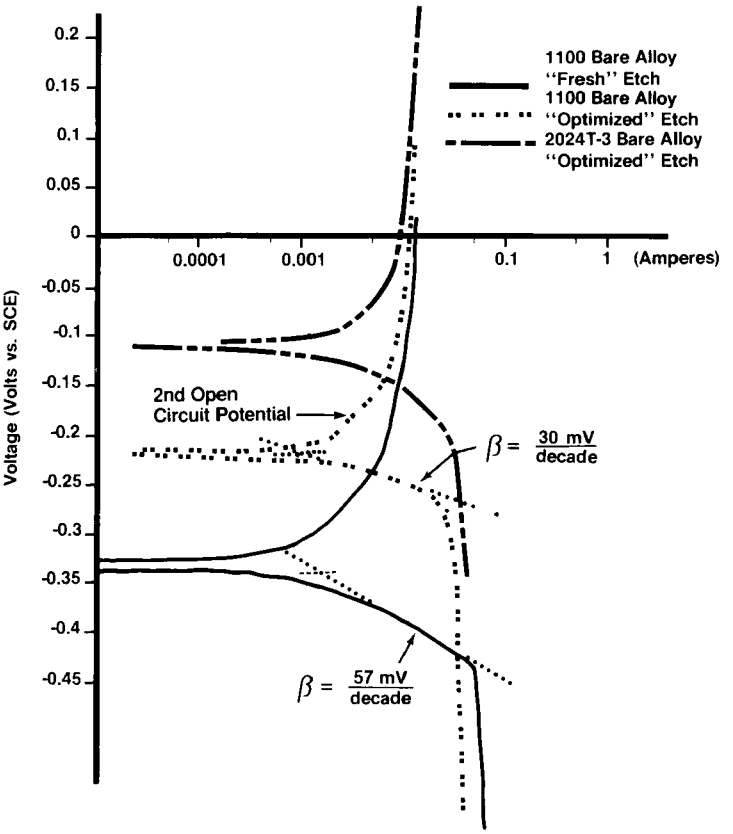

FIGURE 7 Electrochemical polarization curves for (———) 1100 alloy in the "fresh" etch, (--------) 1100 alloy in the "optimized" etch, and (-- ——— --) 2024-T3 bare alloy in the "optimized" etch. Note that for the 1100 alloy the cathodic Tafel slope changes between the two etches and the open circuit potential comes closer to that of the 2024-T3 alloy. There is also the hint of an anodic wave for the 1100 alloy in the "optimized" etch. (From Reference 9a. Reprinted by permission of SAMPE.)

aluminum. The copper plating or dissolution is a charge transfer reaction differing from reaction (3). If reaction (6) takes place in addition to reaction (3), we would expect to see a change in the Tafel slope, as is seen in Figure 7. Indeed, the use of optimized FPL etch solutions which are almost spent results in aluminum surfaces having a coppery hue. It is interesting to note that the oscillations which are displayed in Figure 4 vary approximately between the two open circuit potentials described above. That is, the open circuit potential for clad 2024-T3 alloy or 1100 alloy in the FPL etch is about −290 mV *vs.* SCE while the 2nd open circuit potential observed in the optimized etch for these alloys is about −180 mV. Our polarization data, as shown in Figures 5–7, are consistent with the presence of reactions 1 and 3 being the open circuit condition reactions in the case of the fresh etch. The data also indicate that reaction (6) also must participate at open circuit conditions when copper is present. The open circuit potential for the bare alloy (about −110 mV *vs.* SCE) is above the mixed potential which included reaction (6) and hence does not display the oscillating open circuit potential as observed for the clad and 1100 alloy.

SURFACE CHEMISTRY AND SURFACE MORPHOLOGY

We have carried out measurements of the chemistry of surfaces which were etched under the optimized and fresh EPL etch conditions using Auger Electron Spectroscopy combined with ion sputtering.[15b] The data will be recounted in summary form. We observed that the surface of as-received aluminum is mostly MgO and that the MgO is essentially completely removed by either etch. Electron micrographs clearly show the presence of sparsely placed etch pits. The number of etch pits was much greater in the case of the 2024-T3 bare alloy than in the clad alloy. We observed the segregation of copper at the metal/oxide interface of the bare 2024-T3 alloy as did Venables, *et al.*[3] We observed that the oxide is thicker on the optimized etch surfaces for all alloys investigated, including the bare 2024-T3 alloy. This last finding is particularly difficult to explain in light of the data shown in Figure 2 which indicate that there is little difference between the polarization curves of bare 2024-T3 alloy in fresh or optimized FPL etch solutions, indicating that the reaction rates are similar. Finally, using secondary electron microscopy, we observed in the case of the clad and 1100 alloys in the fresh FPL etch that the oxide on the surface was malformed and discontinuous, while the oxide resulting from the optimized etch looked much like that formed on the bare 2024-T3 alloy in either of the etch solutions. That is, the oxide was porous and corresponded well to the isometric drawings presented by Venables, *et al.*[2a]

SUGGESTED MECHANISM OF OXIDE FORMATION

The proposed mechanism for the effect of seeding of FPL etch solutions is shown in Figures 8, 9 and 10. Figure 8 shows a cross section of a non-copper-containing alloy. Our data indicate that during the etching process the mill oxide, which is mostly MgO, is removed. The oxide reforms in the rinse bath as discussed below. The oxide regrows uniformly, at the same density and location of anodic and cathodic sites that were on the surface before the etch, and remain on the surface after the etch. Figure 9 shows our suggested mechanism for non-copper-containing alloys in the optimized etch. Consistent with our data is the deposition of microscopic metallic copper islands on the surface. These copper islands are small enough to be undetectable by secondary electron microscopy and are also in equilibrium with copper in solution. This copper equilibrium becomes the second open circuit potential as described above and is also the cause of the open circuit potential oscillations. Our most controversial suggestion regarding the mechanism of the etch is that the oxide does not reform in the etch solution, but rather reforms during the rinsing and drying steps. We make this suggestion for the following reasons. Under open circuit conditions the exchange currents, which are a measure of the electrochemical reaction rates at the electrode surfaces, are essentially the same for all of the alloys examined in either the optimized or fresh etch. See Figures 5, 6 and 7. This would indicate that if the reaction taking place in the etch was formation of an anodic oxide, we should see either a diffusion limiting current or an exchange current which increased in the optimized etch. This is not observed. Indeed, the

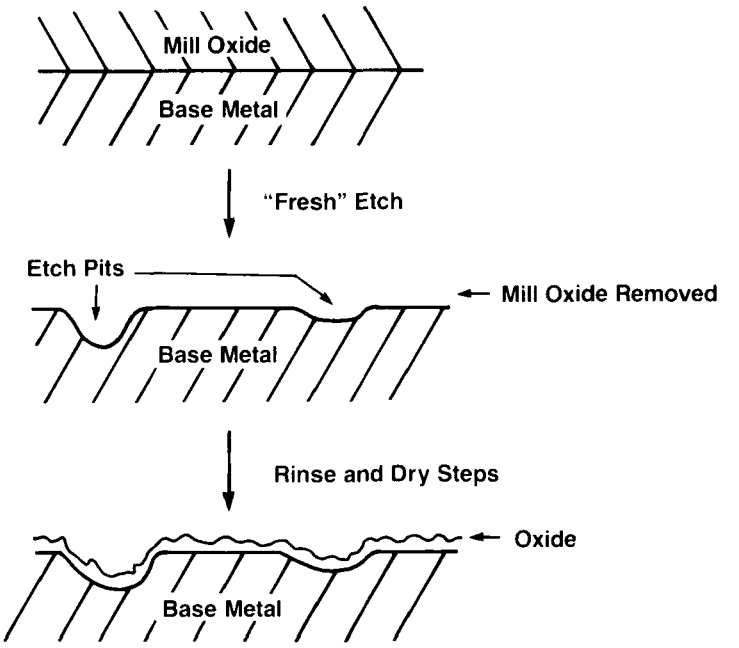

FIGURE 8 Proposed mechanism for clad or non-copper-containing alloys in the "fresh" FPL etch solution.

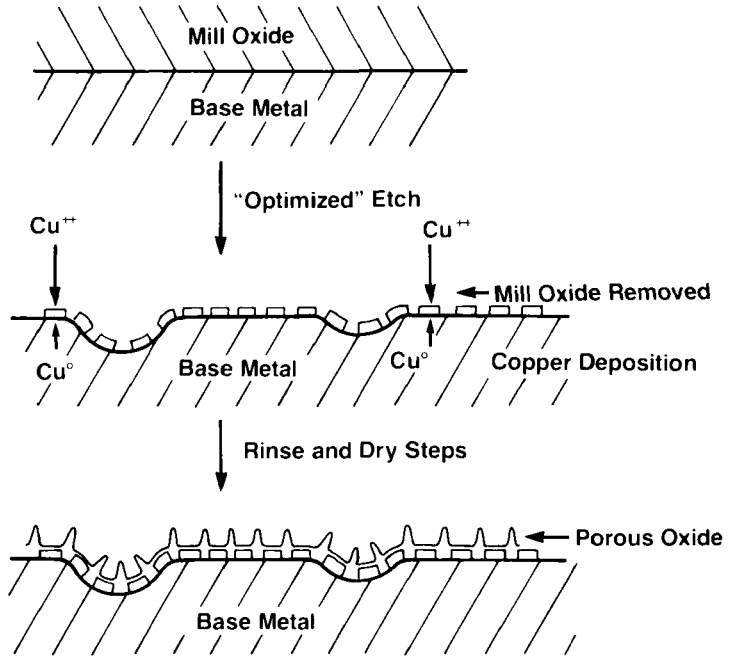

FIGURE 9 Proposed mechanism for clad or non-copper-containing alloys in the "optimized" FPL etch.

portion of the polarization curves which corresponds to anodization is removed by more than 50 mV from the open circuit potential. In the case of the non-copper-containing alloys the oxide reformation is controlled by the microscopic copper islands. That is, each copper site is now a cathode and the aluminum adjacent to the copper is an anode. The electrochemical potential difference between the two sites (>50 mV) is enough to cause anodization to take place on a local scale in the rinse bath, the rate being highest at the edge of the copper island. This causes the porosity that is normally observed for this surface. This also explains the observance of copper segregation at the oxide/metal interface. Figure 10 shows the model for copper-containing alloys. It is well known that a substantial portion of the copper in 2024-T3 alloy is in the form of intermetallics. These intermetallics are known local cathodes[22] and cause the substantial increase in etch pits observed for these alloys. Our model says that since this copper is already in the alloy, it only needs to dissolve from the surface and redeposit in order to form the micro-islands of metallic copper postulated above, *i.e.* the solution is "seeded" locally rather than externally. The only discrepancy between our model and our observations is the increase in oxide thickness for the bare 2024-T3 alloy in the optimized etch. A tenuous explanation is that the introduction of copper into the solution supplants the need for copper to dissolve from the alloy, and that the rate of copper deposition is increased since the dissolution step is not necessary for attainment of copper in solution. This results in a micro-island structure appropriate for formation of thick oxide as in the clad case. Indeed, we observed that the oxide thickness for all of the alloys in the optimized etch was remarkably the same.

Venables, *et al.*[2,3] have clearly shown the effect of oxide morphology on durability of structural adhesive bonds. The model described above can be used to predict

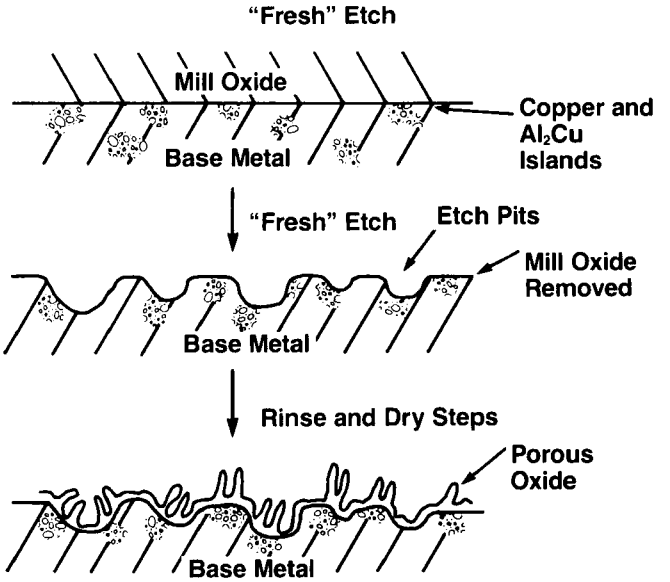

FIGURE 10 Proposed mechanism for copper-containing alloys in the "fresh" FPL etch.

what might happen to oxide morphology, and hence durability, depending upon the type of alloy and the physical etching conditions, as well as the spatial relationship of cut edges to the bonding surfaces on clad alloys. The model would predict the following:

1. If a metallic support frame or rack, especially a copper-containing metallic support, is used to support the metal samples during the etch, the electrochemistry of that support should affect the electrochemistry of the alloy. Conversely, a non-metallic support should have no effect on the electrochemistry and hence no effect on oxide formation.
2. If a clad alloy is being etched in a fresh etch, copper can be dissolved from cut edges and redeposit on the bonding surfaces analogous to the case of the bare alloy. However, because the time in the etch is not infinite, we would expect most of the deposition of copper to occur near the cut edges. Thus a spatial effect on durability should be observed from the edges of the specimen to the interior.
3. There should be no spatial or etching support effects on bare alloy.
4. There should be a great difference in the durability of bonds made in fresh and optimized etch using clad alloys.

These predictions are examined using the Boeing wedge test as described in the next section.

DURABILITY PREDICTIONS

Boeing Wedge Test

The Boeing wedge test[7] was performed using panels that were made of bare or clad 2024-T3 alloy. The panels were 15.24 cm square. Cut edges were left exposed in all experiments. Two types of racking were used in these tests. One was a support frame or rack made from 2024-T3 aluminum while the other was an array of rubber-coated clamps which kept the panels electrically isolated from one another. The etching solutions were either the fresh or optimized FPL etch and, in one experiment, the etch was misformulated to be at the limits of the specification describing its use. EC-3960 primer was used as well as AF-163-2U modified epoxy adhesive (3M). Standard priming and adhesive application and curing conditions were used. After the bonds were made, they were cut into 2.54 cm $\times$ 15.24 cm strips and one side of the specimen was sanded smooth. A wedge made of stainless steel and having a thickness of 0.125" (3.2 mm) was driven into the end of the specimen by means of a hammer and the thus-prepared sample was placed into a chamber of 40°C and condensing humidity. At certain intervals, the samples were removed from the chamber and the length of crack extension was measured by observation under a microscope.

Wedge Test Results

No difference was observed in the durability of adhesive bonds that were made using bare alloy under any of the conditions described above. That is, there was no

spatial effect, no effect of the rack and no effect of the type of etch bath.

The same examination was carried out using 2024-T3 clad alloy. Figure 11 shows the results for a comparison of all of the specimens used in comparing bare *vs.* clad and fresh *vs.* optimized etch. As can be seen, there is little effect of the etchant on the bare alloy but a substantial effect on the clad alloy, as would be predicted from our model. A curious phenomenon was noted when the data were analyzed for the clad alloy. When the standard deviation of the results was determined for the clad alloy samples, it was found to be far greater than the standard deviation for the bare alloy samples. Detailed examination of the data indicated that the greater standard deviation was due to a substantial difference in crack extension resistance between samples, depending upon their location in the original specimen. Figure 12 shows a diagram of the wedge test specimen before it was cut, showing our designations. Figure 13 shows the variation in wedge test results as a function of the specimen position for clad 2024-T3 alloy as defined in Figure 12. As can easily be seen from the data, there is a large difference in the wedge test performance of the samples taken from the edges of the specimen in comparison with those taken from the center of the specimen. The edges provide wedge test results that are approximately the same as that for bare alloy. A similar analysis for bare alloy did not show this difference, in fact the results as a function of position were within each other's standard deviation.

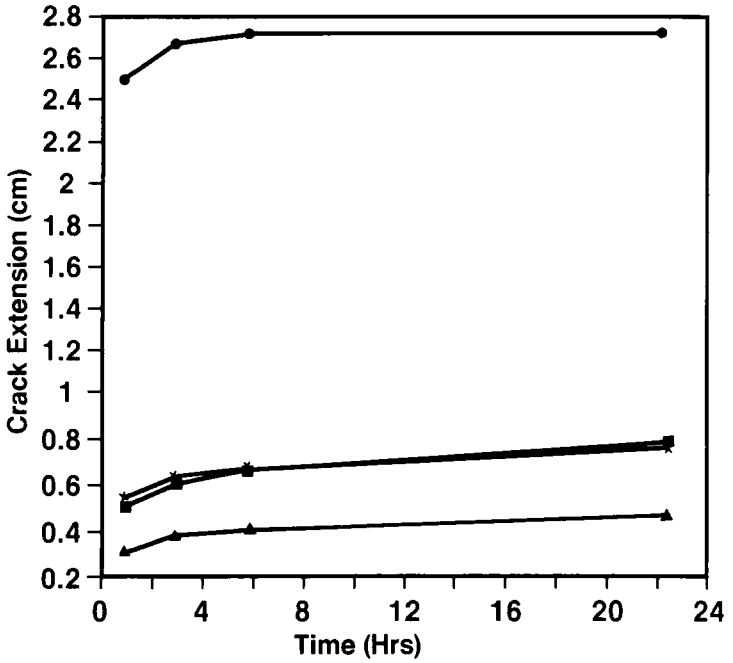

FIGURE 11 Wedge test results for (●) 2024-T3 clad alloy in the "fresh" FPL etch, (▲) 2024-T3 clad alloy in the "optimized" FPL etch, (×) 2024-T3 bare alloy in the "fresh" FPL etch and (■) 2024-T3 bare alloy in the "optimized" FPL etch. Note the substantial difference in the results for the clad alloy between "fresh" and "optimized" etches and the lack of a substantial difference for the bare alloy. (From Reference 9c. Reprinted by permission of Elsevier Publishing Co. and SAMPE.)

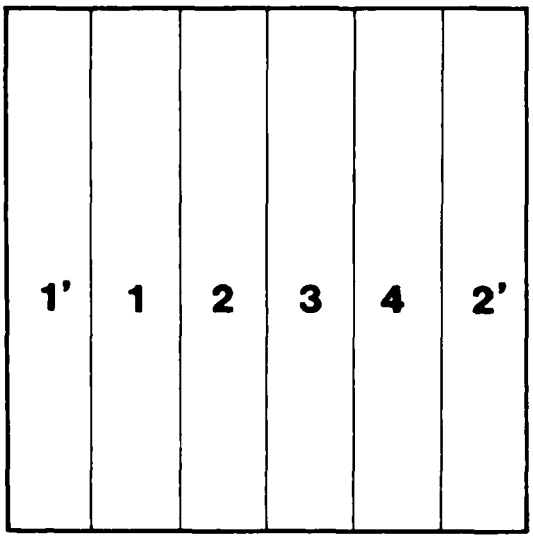

FIGURE 12 Schematic diagram of the sample designations for the wedge test specimens as described in the text and in Figure 13. Note that the "primed" specimens are the edge specimens. (From Reference 9c. Reprinted by permission of Elsevier Publishing Co. and SAMPE.)

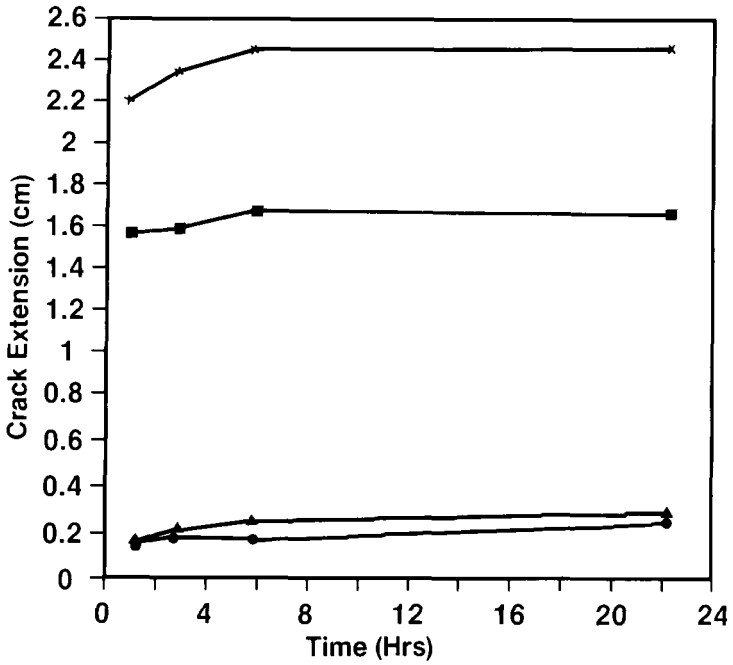

FIGURE 13 Wedge test results showing the performance of bonds made with clad 2024-T3 alloy as a function of the position in the wedge test, as described in Figure 12. (×) positions 2 and 3 from the "fresh" etch, (■) positions 1 and 4 from the "fresh" etch, (▲) positions 2 and 3 from the "optimized" etch, and (●) positions 1 and 4 from the "optimized" etch. Note that the 1 and 4 positions provide better performance than the 2 and 3 positions. The standard deviation of the results is ± 0.4 cm. (From Reference 9c. Reprinted by permission of Elsevier Publishing Co. and SAMPE.)

The above data are supportive of our model. We believe that copper is etched away at the bare edges of the clad alloy sample. This is shown schematically in Figure 14. The copper redeposits at the closest site, which would be the clad metal at the edge. There it forms micro-islands which lead to porous oxide formation. The center of the specimen is too remote from the cut edges and, during the limited time of exposure to the solution, is not exposed to copper; hence, it does not form porous oxide. Unfortunately, time and equipment limitations did not allow us to examine the oxide morphology of the center *versus* edges of the specimens. We did visually observe a difference between the center and edges of the clad alloys etched in the fresh etch. That is, there was an easily observable "halo" extending from the edges of the specimen to about 3.5 cm towards the center. Such halos were not observed for bare alloy in either etch or for the clad alloy in the optimized etch. We believe that the halo was due to porous oxide formation. Indeed, porous oxides are usually visibly different from non-porous and non-oxide-containing surfaces.

In a second set of experiments, we investigated the effect of the type of rack. In this case, we formulated a fresh FPL etch solution that was at the extremes of the formulation. That is, the dichromate level was high and the acid level was low. These results are shown in Figure 15. Once again, a substantial spatial variation is observed but, in addition, the effect of the racking is substantial. Using a conductive copper-containing rack, the wedge test results are substantially better than those obtained using the non-conductive rack. These results also support our mechanism by indicating that the source of copper need not be from the alloy or from the solution but can also be from the rack. These results also indicate that misformulation of the etch to the limits of its formulation can lead to substantially poorer results than at the center point of the formulation. Other test results in the same series of experiments indicated a small effect of the level of toughness of the structural adhesive used for the test, as well as the time of exposure of the unprimed, surface-prepared specimen to 25°C/50% RH. These effects were not as noticeable as those described above.

HISTORICAL PERSPECTIVE

Our results provide some possible reasons for the historical irreproducibility of aluminum adhesive bonds made using FPL etched adherends. The primary reason must have been the prevalence of clad aluminum structures in use in that time period. The poor results led to the phrase "clad is bad" in the aerospace adhesive bonding industry. The use of clad metal is particularly bad because not only is it more sensitive to etch conditions, but once delaminated it provides an ideal site for crevice corrosion in the adhesive bond, accelerated by the electrochemical difference between the cladding and the bare metal. A second reason for the irreproducibility may have been that the edges of a fresh FPL etched clad metal specimen would provide proper oxide structure but the interior would not. Thus, the large panels normally used in the aerospace industry could have demonstrable differences in durability depending upon whether the adhesive bonds were made near cut outs or cut edges or if they were remote from cut edges. In addition, the usual method

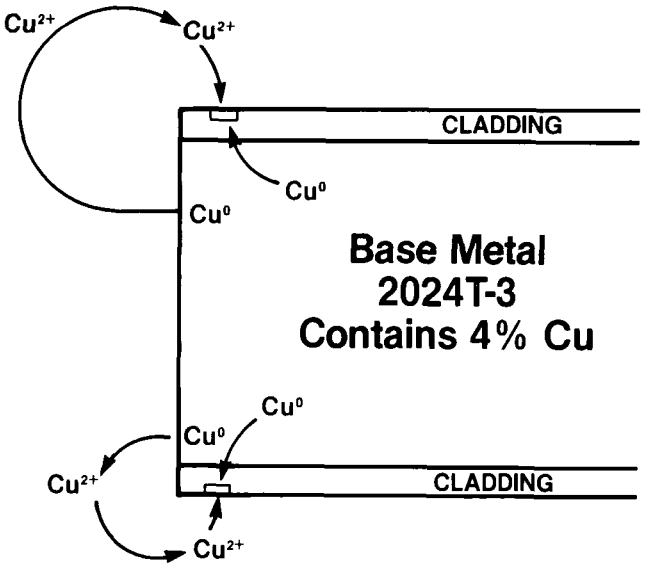

FIGURE 14 Schematic diagram showing the proposed mechanism for the formation of porous oxide on the edges of clad 2024-T3 alloy leading to the spatial variation of wedge test performance and the "halo" effect.

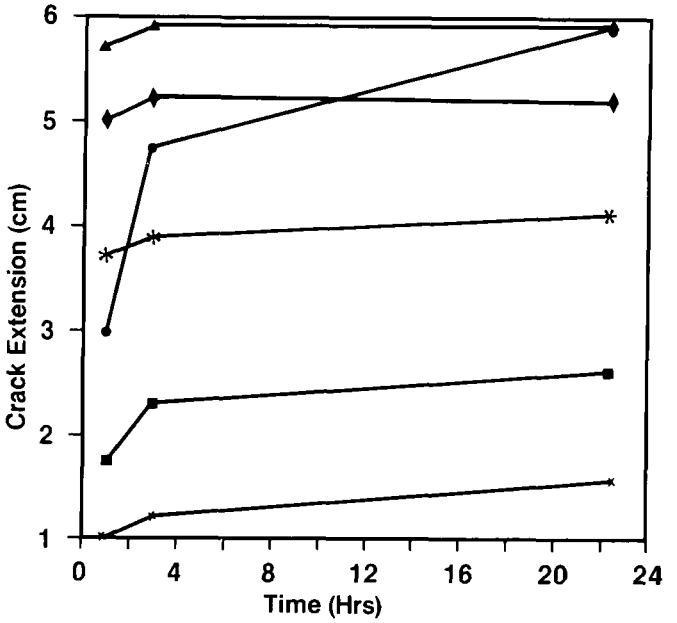

FIGURE 15 Wedge test results showing the performance of bonds made with clad 2024-T3 alloy as a function of position and type of rack used to support the specimens in the bath. Bath formulation was made to be a "worst case" situation with high dichromate and low acid content. (×) positions 1′, 2′, conductive rack, (■) positions 1′, 2′, nonconductive rack, (*) positions 1, 4, conductive rack, (●) positions 2, 3, nonconductive rack, (♦) positions 2 and 3, conductive rack and (▲) positions 2, 3, nonconductive rack. Note that the center specimens performed most poorly and samples made using the nonconductive rack performed more poorly than those made with the conductive rack. (From Reference 9c. Reprinted by permission of Elsevier Publishing Co. and SAMPE.)

of quality control in an adhesive bonding operation is to process small panels in addition to the large panels and to test those small panels destructively to provide certification for the large panels. The spatial discrepancy that we have discovered would have provided small panels that seemed to be durable because the edges and the interior of the panel were close together, while a large panel would not be durable because much of the adhesive bonded area would be remote from the cut edges. The type of racking could also have had an effect, as well as the proximity of the panels during the etching process. We have also shown that variation within the formulation parameters of the etch could have had large effects on durability.

SUMMARY

By means of electrochemical methods, modern surface analytical techniques and wedge tests, we have examined the phenomenon of durability of adhesive bonds made with aluminum adherends etched by the FPL process. We have proposed a mechanism for the formation of a porous oxide based upon the deposition of micro-islands of copper during the etching process. The proposed mechanism and its effect on oxide formation is predictive of effects on durability of adhesive bonds. These effects were then used to provide a historical perspective on the irreproducibility of the durability of adhesively bonded aerospace structures manufactured during the 1960's.

Acknowledgements

The author would like to acknowledge the excellent work of the co-authors of the several original papers which have been combined to form this review: S. Sugii, T. H. Wilson, Jr. and S. H. Lundquist. In addition, the author would like to express his thanks to the Society for Advancement of Materials and Process Engineering (SAMPE), Plenum Press and the Elsevier Publishing Co. for their kind permission to republish this information.

References

1. J. C. McMillan, in *Bonded Joints and Preparation for Bonding,* AGARD Lecture Series No. 102 (Harford House, London, UK, 1979).
2. a. J. D. Venables, *J. Material Sci.,* **19,** 2431 (1984).
   b. S. P. Kodali, R. C. Curley, L. Cottrell, B. M. Ditchek, D. K. McNamara, J. D. Venables, *Proc. 13th Nat'l SAMPE Tech Conference* (SAMPE, Covina, CA, USA, 1981), pp. 676–684.
   c. J. D. Venables, in *Adhesion, Vol. 7* K. W. Allen, Ed (Applied Science Publishers, London, 1983), pp. 87–93.
   d. J. D. Venables, D. K. McNamara, J. M. Chen, T. S. Sun, R. L. Hopping, *Appl. Surf. Sci.,* **3,** 88 (1979).
   e. T. S. Sun, J. M. Chen, J. D. Venables, R. L. Hopping, *Appl. Surf. Sci.,* **1,** 202 (1978).
3. L. F. Cottrell, D. L. Trawinski, S. P. Kodali, R. C. Curley, D. K. McNamara, J. D. Venables, *Proc. 27th Nat'l SAMPE Symposium* (SAMPE, Covina, CA, USA, 1982), pp. 44–52.
4. H. W. Eichner, *Forest Products Laboratory Report #1842,* April 1, 1954, Madison, WI, USA.
5. L. H. Sharpe, *Appl. Polym. Symp.* **3,** 353 (1966).
6. A. W. Bethune, *SAMPE J.,* August, 1975, pp. 4–10.
7. a. J. A. Marceau, Y. Moji and J. C. McMillan in *Proc. 21st National SAMPE Symposium and Exhibition* (SAMPE, Covina, CA, USA, 1976).
   b. ASTM Standard Test Method D-3762 (Am. Soc. for Testing & Matls., Philadelphia, PA, USA).

8. J. A. Marceau, R. H. Firminhac, Y. Moji, U. S. Patent 4, 127, 451, Issued Nov. 28, 1978, Assigned to Boeing Co.
9. A. W. Smith, *J. Electrochem. Soc.*, **120,** 1551 (1973).
10. P. F. A. Bijlmer, *Metal Finishing,* p. 34 (December, 1971).
11. W. J. Russell, E. A. Garnis, *SAMPE Quarterly,* p. 5 (April, 1976).
12. R. F. Wegman, W. M. Bodnar, M. J. Bodnar, M. J. Barbarisi, *SAMPE J.*, p. 35 (Oct/Nov, 1967).
13. W. T. McCarvill, J. P. Bell, *J. Appl. Polym. Sci.*, **18,** 343 (1974).
14. L. Kozma, I. Olefjord, *Materials Science and Tech.*, **3,** 860 (1987).
15. a. A. V. Pocius, in *Proc. 28th Nat'l. SAMPE Symposium, April 1983,* Anaheim, CA, pp. 1127–1141.
    b. A. V. Pocius, in *Adhesion Aspects of Polymeric Coatings* K. L. Mittal, Ed. (Plenum Press, New York, USA, 1983), pp. 173–192.
    c. A. V. Pocius, T. H. Wilson, S. H. Lundquist, S. Sugii, in Progress in Advanced Materials: Durability, Reliability and Quality Control, G. Bartelds and R. J. Schliekelmann, Eds. (Elsevier Science Publishers, Amsterdam, 1985), pp. 71–81.
16. D. A. Jones, *Ind. Eng. Chem. Prod. Res. Dev.*, **11,** 12 (1972), and references contained therein.
17. a. *Metals Handbook, 8th Edition,* T. Lyman, Ed. (American Society for Metals, Metals Park, OH, USA, 1961), p. 925.
    b. *Metals Handbook, 9th Edition,* W. H. Cubbard, DIR (American Society for Metals, Metals Park, OH, USA, 1979), pp. 45, 74, 210–211.
18. a. U. F. Franck. *Angewandte Chemie, Intl. Ed.*, **17,** (1978).
    b. H. D. Dorfler, E. Miller, *J. Electroanal. Chem.*, **135,** 37 (1982).
    c. G. Nicolis, J. Portnow, *Chem. Rev.*, **73,** 365 (1973).
    d. P. C. Jordan, *Chemical Kinetics and Transport* (Plenum Press, New York, USA, 1979), Ch. 7.
    e. N. D. Thomashov, E. N. Ustinskii, G. P. Chemova, *Electrokhimiya (USSR),* **17,** 969 (1981).
19. K. J. Vetter, *Electrochemical Kinetics, Theory and Experimental Aspects* (Academic Press, New York, USA, 1967), pp. 786–789.
20. J. K. Hawkins, H. S. Isaacs, S. M. Heald, J. Tranquada, G. E. Thompson and G. C. Wood, in *Proc. Electrochem. Soc.* (Aluminum Surface Treatment Technology), **86–11,** 345–54, 1986.
21. K. J. Vetter, *ibid,* pp. 732–745.
22. A. Datta, R. A. Pethrick, S. Afrossman, *J. Adhesion,* **15,** 13 (1982).